

Keywords

RC Beams,
Strengthening,
Flexural Capacity,
FRP,
NSM,
Design

Received: April 8, 2017

Accepted: April 27, 2017

Published: July 5, 2017

Flexural Analysis of RC Rectangular and T Beams Strengthened with NSM FRP Reinforcement

Brahim Bousalem¹, Riad Benzaid^{2, *}, Nasr Eddine Chikh¹,
Habib-Abdelhak Mesbah³

¹LMDC Laboratory, Department of Civil Engineering, Frères Mentouri University, Constantine, Algeria

²L.G.G. Laboratory, Mohammed Seddik Benyahia University, Jijel, Algeria

³L.G.C.G.M., INSA de Rennes, IUT Université de Rennes, Rennes, France

Email address

benzaid_riad@yahoo.fr (R. Benzaid)

*Corresponding author

Citation

Brahim Bousalem, Riad Benzaid, Nasr Eddine Chikh, Habib-Abdelhak Mesbah. Flexural Analysis of RC Rectangular and T Beams Strengthened with NSM FRP Reinforcement. *International Journal of Civil Engineering and Construction Science*. Vol. 4, No. 1, 2017, pp. 1-10.

Abstract

In recent years, the repair of damaged reinforced concrete members using Near surface Mounted (NSM) technique has proven its success in structural rehabilitation and upgrade. The NSM technique using carbon fiber reinforced polymer (FRP) laminate strips is now a well-established process for the strengthening/retrofit of reinforced concrete structures. The amount of analytical studies for predicting the flexural capacity of RC beams strengthened with carbon FRP laminates using NSM technique is constantly rising to the point that a design guidelines to such applications were introduced. This paper investigates the flexural behavior of reinforced concrete beams strengthened with carbon FRP laminates using NSM technique. The objective of this study is to provide an efficient and direct computational analysis for the evaluation of the flexural strength capacity of the carbon FRP reinforced concrete sections. The analysis is based on common principles of equilibrium equation and compatibility of strains of simply and doubly reinforced rectangular and "T" concrete sections. To ensure ductile failures, expressions for upper and lower values of the characteristic carbon FRP reinforcement ratios were derived using the CBA 93 model for concrete. Design nomographs to materialize the implementation of the procedure were developed and a parametric study was performed. The solution, using the developed equations is compared to some experimental data available in the literature. The comparison showed the validity and the effectiveness of the present design equations in accurately estimating the flexural capacity of simply and doubly reinforced concrete rectangular and "T" sections strengthened with carbon FRP laminates strips.

1. Introduction

The rehabilitation of under-strengthened or damaged reinforced concrete members by external bonding of Fiber-Reinforced Polymers (FRP) materials have been used extensively and becoming increasingly popular in the world of construction. The use of FRP sheets and strips for the repair of different constructional elements offers several advantages namely resistance to corrosion, light weight, high strength and facility in handling. Experimental studies [1-8] have shown that the flexural strength capacity of concrete beams is significantly increased by the use of the FRP on the surface of the

elements to be strengthened. The increase depends on many factors such as longitudinal steel ratio, FRP ratio, concrete compressive strength, FRP mechanical properties and the level of damage.

One of the popular methods in the strengthening of reinforced concrete (RC) beams is by providing externally bonded reinforcement (EBR) made of fiber-reinforced polymer (FRP) laminates for additional flexural resistance. However, many tests carried out on RC beams strengthened for flexure with externally bonded FRP materials indicated low efficiency of this technique, caused by premature FRP debonding failure [8-12]. Furthermore, the main deficiencies in the performance of EBR technique are susceptibility to damage from collision, fire, temperature variation, ultraviolet rays, high possibility of brittle failure mode that it mostly due to premature debonding of FRP sheet from the concrete substrate and vulnerability of FRP materials against the environmental conditions. Near surface mounted (NSM) technique has become promising and attractive for flexural strengthening of RC beams. The NSM technique consists in applying carbon fiber-reinforced polymer (CFRP) laminate strips into slits opened in the concrete cover of the elements to be strengthened. A normal cold cured epoxy based adhesive is used to bond the CFRP laminate strips to concrete. Due to better anchorage of embedded NSM FRP reinforcement, this technique has been significantly more efficient than EBR system [7, 8, 11].

Many experimental tests indicated benefits of NSM technique such as: (a) increase in the load carrying capacity of RC members and easy to apply [8, 11-15], (b) postponing or even eliminating the debonding phenomenon, (c) possibility of using this technique in the negative moment region of flexural frames, (d) preserving strengthening materials against severe environmental conditions (such as: mechanical impacts, abrasion, fire, freeze/thaw cycles and UV radiations) [11, 15]. Also in this technique, the strengthening materials are embedded in the concrete cover and are confined with the concrete sides of the grooves, which further eliminates the debonding phenomenon. However, the performance of the NSM technique seems to be controlled entirely by the bond behavior of the interface laminate adhesive-concrete [16-20].

Several analytical techniques [21-28] for evaluating the ultimate flexural capacity of concrete section strengthened by FRP laminates have been reported. In this study, a straightforward analytical procedure for the flexural analysis of reinforced concrete rectangular and "T" sections strengthened with FRP reinforcement is presented.

2. Section Analysis

2.1. Failure Modes

The possible failure modes of beams flexurally strengthened with NSM CFRP reinforcement are of two types: those of conventional RC beams, including concrete

crushing or NSM CFRP rupture generally after the yielding of internal steel bars, for which the composite action between the original beam and the NSM CFRP is practically maintained up to failure, and "premature" debonding failure modes which involve the loss of this composite action. Although debonding failures are less likely a problem with NSM CFRP compared with externally bonded FRP, they may still significantly limit the efficiency of this technology.

In existing research on NSM-FRP reinforcement, FRP bars of various shapes have been used as well as narrow strips. In particular, the latter have been shown to be the least prone to debonding from the concrete substrate [29-31], for two main reasons:

- They maximize the ratio of surface to cross-sectional areas, which minimizes the bond stresses associated with a given tensile force in the FRP reinforcement;
- The normal stresses accompanying the tangential bond stresses, which in the case of NSM round bars tend to split the epoxy cover and the surrounding surface layer of concrete, act in this case mainly towards the thick lateral concrete so that splitting failure becomes less likely [32, 33].

When the FRP NSM system is properly designed, the expected failure modes are the concrete crushing and steel yielding, steel yielding and FRP rupture or steel yielding and FRP debonding. The internal cross-section equilibrium is achieved by the balance between concrete in compression and the contribution of both longitudinal steel and FRP in tension. Hence, the most efficient design solution will be the one which explores more efficiently the reinforcement materials (steel and FRP) thus conducting to concrete crushing after longitudinal steel yielding being the FRP safely close to failure. This leads to a ductile failure, with all materials being used up to their capacity. The last two failure modes (steel yielding with FRP either in rupture or debonding) are the most difficult to prevent because the existing prediction models of bond strength are not robust enough yet. As a result, there is significant uncertainty regarding the definition of the critical failure mode, hindering the quality of strength predictions even for concrete crushing failures. In fact, if it was possible to predict the highest load that the FRP can attain without debonding, then it would be possible to design the FRP system not failing in tension. Then, it would also be possible to check, by the internal cross-section equilibrium, whether or not the concrete strength allows full load transfer [15, 34]. In practice, if necessary, provision of adequate end anchorages at the ends of the FRP strips and at critical sections along the span such as: U, L and X shaped wrappings can contribute to postpone or even eliminate the debonding phenomenon [35, 36].

In the present analysis, it is assumed that the beam is properly detailed so as to preclude debonding failure modes.

2.2. Assumptions of Present Analysis

The design equations presented herein are based on the following assumptions:

- a) Linear strain distribution across the section depth.

- b) Compressive force in concrete, at crushing, is determined by an equivalent rectangular stress block as proposed by the CBA 93 [37]. The ultimate compressive strain in concrete is assumed to be 0.0035.
- c) Tensile stresses in concrete, at ultimate strength, are ignored.
- d) Reinforcing steel is assumed to have elastic-perfectly plastic response.
- e) FRP behaves linearly up to brittle failure since its fibres are aligned with the beam axis.
- f) Perfect FRP strip bond is considered for strain compatibility equations.
- g) The governing failure mode is concrete crushing, preceded by steel yielding, prior to FRP rupture. A minimum FRP ratio is formulated to ensure this failure mode.

3. Rectangular Section

The procedure formulated in this study utilizes the direct principles of equilibrium equation and compatibility of strains of simply and doubly reinforced rectangular and "T" concrete sections in order to determine the flexural strength design of FRP-strengthened beams. They differ from the current state of the art iterative procedure which often leads to tedious calculations. It is assumed also that the beam is designed so that shear or debonding should not precede other type failure modes.

Referring to Figure 1, the force equilibrium condition for the tension failure mechanism in a singly or doubly reinforced concrete beam is as follows:

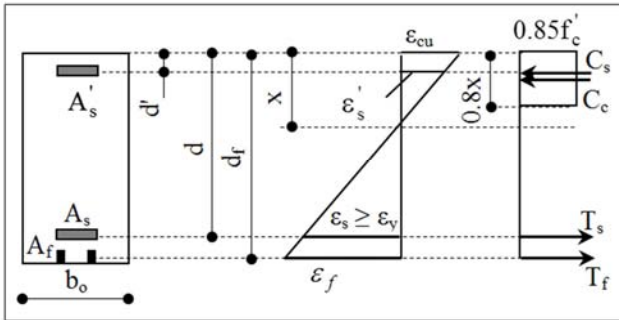


Figure 1. Doubly reinforced rectangular cross-section with strain distribution and force profile.

3.1. Case of Simply Reinforced Concrete Section (Assuming: $A'_s = 0$)

$$0.85f'_c \times 0.8b_o x = A_s f_y + A_f f_f \quad (1)$$

The FRP steel ratio can be obtained from equation 1 in a non dimensional form as:

$$\rho_f = 0.68\alpha \frac{f'_c}{f_f} - \rho_s \frac{f_y}{f_f} \quad (2)$$

The expression of the ultimate moment of resistance may be obtained by summing the moments of the forces acting on cross section about the centroid of the FRP tension steel:

$$M_r = 0.85f'_c \times 0.8b_o x (d_f - 0.4x) - A_s f_y (d_f - d) \quad (3)$$

Rewriting in non-dimensional form leads to:

$$\mu_r = 0.68\alpha(1 - 0.4\alpha) - \rho_s \frac{f_y}{f'_c} \left(1 - \frac{d}{d_f}\right) \quad (4)$$

3.2. Case of Doubly Reinforced Concrete Section ($A'_s \neq 0$)

According to Figure 1, the force equilibrium condition gives:

$$0.85f'_c \times 0.8b_o x + A'_s f'_s = A_s f_y + A_f f_f \quad (5)$$

Or, in non dimensional form:

$$\rho_f = \frac{1}{f_f} \left[0.68\alpha f'_c + \rho'_s f'_s - \rho_s f_y \right] \quad (6)$$

The sum the moments of the forces acting on cross section about the centroid of the FRP tension steel is:

$$M_r = 0.85f'_c \times 0.8b_o x (d_f - 0.4x) - A_s f_y (d_f - d) + A'_s f'_s (d_f - d') \quad (7)$$

The non dimensional moment is expressed as:

$$\mu_r = 0.68\alpha(1 - 0.4\alpha) + \rho'_s \frac{f'_s}{f'_c} \left(1 - \frac{d'}{d_f}\right) - \rho_s \frac{f_y}{f'_c} \left(1 - \frac{d}{d_f}\right) \quad (8)$$

where $\rho_f = \frac{A_f}{b_o d_f}$, $\rho_s = \frac{A_s}{b_o d_f}$, $\alpha = \frac{x}{d_f}$ and $\mu_r = \frac{M_r}{b_o d_f^2 f'_c}$.

Using strain compatibility, the strain in the FRP strip ϵ_f is given by:

$$\epsilon_f = \frac{d_f - x}{x} \epsilon_{cu} \quad (9)$$

Considering that $\alpha = \frac{x}{d_f}$, the above equation is rewritten as follows:

$$\epsilon_f = \left(\frac{1}{\alpha} - 1 \right) \epsilon_{cu} \quad (10)$$

Where ϵ_f is the FRP strain at failure, considering zero initial concrete strain during strengthening, the actual tensile stress in FRP strip is can be expressed as:

$$f_f = \varepsilon_f E_f = \left(\frac{1}{\alpha} - 1 \right) \varepsilon_{cu} E_f \quad (11)$$

3.3. Minimum FRP Reinforcement Ratio in Simply RC Rectangular Section

As stated earlier, the desired mode of failure is yielding of steel reinforcement followed by concrete crushing prior to FRP rupture. The latter cannot be guaranteed unless the FRP stress, at concrete crushing, is lower than its design ultimate strength f_{fu} . This may be conveniently prescribed by keeping the FRP ratio greater than that minimum needed to attain FRP design ultimate strength (f_{fu}) upon concrete crushing.

Accordingly, the strain compatibility and force equilibrium equations are used to define such a ratio. If Eq. (2) above yields a lower FRP ratio, the minimum should be obviously used to avoid any possible FRP rupture failure. Thus Eq. (2) is used to provide the minimum FRP ratio by defining the corresponding strain distribution where:

$$\frac{\varepsilon_{cu}}{x_{\min}} = \frac{\varepsilon_{cu} + \varepsilon_{fu}}{d_f} \Rightarrow x_{\min} = \frac{0.0035}{0.0035 + \varepsilon_{fu}} d_f \quad (12)$$

$$0.85 f'_c b_o 0.8 x_{\min} = A_s f_y + A_{f \min} f_{fu} \Rightarrow \rho_{f \min} = 0.68 \frac{f'_c}{f_{fu}} \frac{x_{\min}}{d_f} - \rho_s \frac{f_y}{f_{fu}} \quad (13)$$

Except for lightly reinforced sections, the second term of Eq. 13 is typically larger than the first term, yielding negative values of $\rho_{f \min}$ which indicate that reaching FRP design ultimate strength (f_{fu}) prior to concrete crushing is not possible.

3.4. Maximum FRP Reinforcement ratio in Simply RC Rectangular Section

To ensure ductile failure, steel yielding needs to take place prior to concrete compression failure. This can only happen if the area of FRP strip is kept lower than that causing balanced failure (i.e. simultaneous yielding of steel and crushing of concrete). Thus, the maximum FRP ratio may be expressed in terms of the difference between the balanced and actual steel ratios of the original un-strengthened section, as follows:

$$\frac{\varepsilon_{cu}}{x_{bal}} = \frac{\varepsilon_{cu} + \varepsilon_y}{d} \Rightarrow x_{bal} = \frac{0.0035}{0.0035 + \frac{f_e}{E_s}} d = \frac{700}{700 + f_e} d \quad (14)$$

$$\frac{\varepsilon_{cu}}{x_{bal}} = \frac{\varepsilon_{cu} + \varepsilon_{f \text{ bal}}}{d_f} \Rightarrow \varepsilon_{f \text{ bal}} = \left(\frac{d_f}{x_{bal}} - 1 \right) \varepsilon_{cu} \quad (15)$$

$$\varepsilon_{f \text{ bal}} = 0.0035 \left(\frac{700 + f_e}{700} \frac{d_f}{d} - 1 \right)$$

$$0.85 f'_c 0.8 x_{bal} b_o = A_s f_y + A_{f \text{ bal}} E_f \varepsilon_{f \text{ bal}} \quad (16)$$

Substituting Eqs. (14) and (15) into Eq. (16) and rearranging:

$$\frac{E_f \varepsilon_{f \text{ bal}}}{f_y} \rho_{f \text{ bal}} = 0.68 \frac{f'_c}{f_y} \left(\frac{700}{700 + f_e} \frac{d}{d_f} \right) - \rho_s \Rightarrow \rho_{f \text{ bal}} = \frac{f_y}{f_{f \text{ bal}}} (\rho_{s \text{ bal}} - \rho_s) \quad (17)$$

where $\rho_{f \text{ bal}} = \frac{A_{f \text{ bal}}}{b_o d_f}$, $\varepsilon_{f \text{ bal}}$ is given by Eq. (15).

$$\rho_f \leq \rho_{f \text{ max}} = 0.75 \rho_{f \text{ bal}} - \rho_s \frac{f_y}{f'_c} \left(1 - \frac{d}{d_f} \right) \quad (18)$$

It is clear from Eq. (17) that cross-sections originally reinforced with the balanced steel ratio cannot exhibit a pseudo-ductile failure when strengthened with FRP strips. Fortunately, in current code practice the steel ratio ρ_s is limited to 75% of the balanced steel ratio according to the ACI 318-02 [38]. This same fraction may be used here to limit the maximum FRP ratio so that the same type of pseudo-ductile failure is ensured:

$$\rho_{s \text{ max}} = 0.75 \rho_{s \text{ bal}}, \rho_f \leq \rho_{f \text{ max}} = 0.75 \rho_{f \text{ bal}} \quad (19)$$

3.5. Minimum and Maximum FRP Reinforcement Ratio in Doubly RC Rectangular Section

The derivation of the minimum and maximum FRP ratios follows analogous steps to those of Eqs. (12)–(17) yielding the following expressions

- Minimum FRP ratio:

$$\rho_{f \min} = 0.68 \frac{f'_c}{f_{fu}} \frac{x_{\min}}{d_f} + \rho'_s \frac{f'_s}{f_{fu}} - \rho_s \frac{f_y}{f_{fu}} \quad (20)$$

where x_{\min} is given by Eq. (12), and $f'_s = 700 \frac{x_{\min} - d'}{x_{\min}}$ (21)

- Maximum FRP ratio:

$$\rho_{f \text{ max}} = \frac{1}{f_{f \text{ bal}}} (0.75 \rho_{bal} + \rho'_s f'_{s \text{ bal}} - \rho_s f_y) \quad (22)$$

where $f_{f \text{ bal}} = E_f \left(0.0035 \frac{d - x_{bal}}{x_{bal}} \right) \leq f_{fu}$ (23)

$$\text{and } f'_{s \text{ bal}} = 700 \frac{x_{bal} - d'}{x_{bal}} \leq f_y \quad (24)$$

4. "T" Section

"T" sections may be analyzed as a rectangular section if

the neutral axis depth x at the ultimate state falls within the slab (flange). In this case, the section is calculated with a compression face width equal to the effective flange width b . Therefore the next part focuses on cases where the neutral axis depth extends outside the flange thickness h_o . Referring to Figure 2, the force equilibrium condition for the tension failure mechanism and the sum of moments about the tension force in the FRP reinforcement yields to:

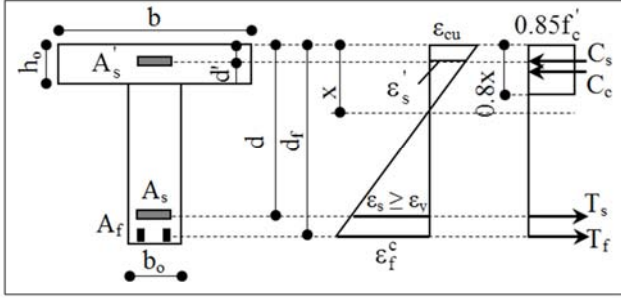


Figure 2. Doubly reinforced T-section with strain distribution and force profile.

4.1. Case of Simply Reinforced Concrete "T" Section (Assuming: $A'_s = 0$)

$$0.85f'_c [0.8b_o x + (b - b_o)h_o] = A_s f_y + A_f f_f \quad (25)$$

The FRP steel ratio can be obtained from Eq. (25) in a non-dimensional form as:

$$\rho_f = \frac{f'_c}{f_f} \left[0.68\alpha + 0.85 \frac{h_o}{d_f} \left(\frac{b}{b_o} - 1 \right) \right] - \rho_s \frac{f_y}{f_f} \quad (26)$$

where ρ_f , ρ_s and α as defined above.

$$M_r = 0.85f'_c (b - b_o) h_o \left(d_f - \frac{h_o}{2} \right) + 0.85f'_c \times 0.8b_o x \left(d_f - 0.4x \right) - A_s f_y (d_f - d) \quad (27)$$

Writing equation (27) in a non-dimensional form leads to:

$$\mu_r = 0.85 \left(\frac{b}{b_o} - 1 \right) \frac{h_o}{d_f} \left(1 - \frac{h_o}{2d_f} \right) + 0.68\alpha (1 - 0.4\alpha) - \rho_s \frac{f_y}{f'_c} \left(1 - \frac{d}{d_f} \right) \quad (28)$$

$$\text{with } \mu_r = \frac{M_u}{b_o d_f^2 f'_c}$$

4.1.1. Minimum FRP Reinforcement Ratio in Simply Reinforced "T" Section

The same considerations indicated for rectangular sections apply for "T" section, thus the minimum FRP ratio is given by:

$$\rho_{f \min} = 0.85 \frac{f'_c}{f_{fu}} \left[\frac{0.8x_{\min}}{d_f} + \frac{h_o}{d_f} \left(\frac{b}{b_o} - 1 \right) \right] - \rho_s \frac{f_y}{f_{fu}} \quad (29)$$

where x_{\min} is given by Eq. (12).

4.1.2. Maximum FRP Reinforcement Ratio in Simply Reinforced "T" Section

A similar procedure for determining ρ_f^{\max} is utilized for "T" sections. Two cases are considered:

- The neutral axis falls within the flange ($x \leq 1.25h_o$) Eq.

14 can be used to calculate ρ_f^{\max} after replacing the beam web width b_o with the effective flange width b .

- The neutral axis falls outside within the flange ($x > 1.25h_o$) Eq. 14 can be used to calculate ρ_f^{\max} after replacing the beam web width b_o with the effective flange width b .

$$A_{f \max} = \frac{1}{f_{f \text{ bal}}} (0.75C_c - A_s f_y) \quad (30)$$

$$\text{with } C_c = 0.85f'_c [0.8x_{\text{bal}}b_o + h_o(b - b_o)]$$

Rearranging Eq. (30) in non-dimensional form:

$$\rho_{f \max} = \frac{0.75f'_c}{f_{f \text{ bal}}} \left[\frac{0.68x_{\text{bal}}}{d_f} + 0.85 \frac{h_o}{d_f} \left(\frac{b}{b_o} - 1 \right) \right] - \rho_s \frac{f_y}{f_{f \text{ bal}}} \quad (31)$$

where x_{bal} and $f_{f \text{ bal}}$ are respectively given by Eqs. (14) and (23).

4.2. Case of Doubly Reinforced Concrete "T" Section

The equations governing the FRP strengthening design for doubly reinforced sections are similar to those of Eqs. (25–28) with the contribution of the compression steel included. The strain compatibility is used to define the compressive steel strain, Figure 2:

$$\frac{\epsilon_{cu}}{x} = \frac{\epsilon_{cu} - \epsilon'_s}{d'} \Rightarrow \epsilon'_s = 0.0035 \left(1 - \frac{\delta'}{\alpha} \right) \quad (32)$$

$$\text{with } \delta' = \frac{d'}{d_f}$$

Using the force equilibrium and the sum of moments about the centroid of the FRP steel tension force, we obtain the following expressions:

$$0.85f'_c [0.8b_o x + (b - b_o)h_o] + A'_s f'_s = A_s f_y + A_f f_f \quad (33)$$

The same expression in non-dimensional form,

$$\rho_f = \frac{f'_c}{f_f} \left[0.68\alpha + 0.85 \frac{h_o}{d_f} \left(\frac{b}{b_o} - 1 \right) \right] + \rho'_s \frac{f'_s}{f_f} - \rho_s \frac{f_y}{f_f}$$

$$\rho_f = \rho_{f \sin gly} + \rho'_s \frac{f'_s}{f_f} \quad (34)$$

$$M_r = 0.85 f'_c (b - b_o) h_o \left(d_f - \frac{h_o}{2} \right) + 0.85 f'_c \times 0.8 b_o x \left(d_f - 0.4 x \right) + A'_s f'_s \left(d_f - d' \right) - A_s f_y \left(d_f - d \right) \quad (35)$$

In non-dimensional form,

$$\mu_r = 0.85 \left(\frac{b}{b_o} - 1 \right) \frac{h_o}{d_f} \left(1 - \frac{h_o}{2 d_f} \right) + 0.68 \alpha (1 - 0.4 \alpha) + \rho'_s \frac{f'_s}{f'_c} \left(1 - \frac{d'}{d_f} \right) - \rho_s \frac{f_y}{f'_c} \left(1 - \frac{d}{d_f} \right) \quad (36)$$

Equation (34) may be directly solved for α if the compression steel has yielded. f'_s is substituted by f_y assuming that $\epsilon'_s > \epsilon_y$. The value of α obtained is then substituted into Eq. (32) to verify this yielding. If yielding actually takes place, the solution is complete. Otherwise, f'_s is obtained by Eq. (37), then substituted into Eq. (31) resulting in a cubic expression, which may also be directly solved for α using a computer programming.

$$f'_s = 700 \left(1 - \frac{d'}{\alpha d_f} \right) \quad (37)$$

Once α is found as the lowest positive root of Eq. (31), ρ_f is determined by Eq. (29). The complete procedure is summarized in the flowchart represented in Figure 3.

The total FRP ratio ρ_f needs to satisfy the minimum and maximum limits. The same analogous steps used for doubly RC rectangular section are employed.

4.2.1. Minimum FRP Reinforcement Ratio in Doubly RC "T" Section

$$\rho_{f \min} = \frac{f'_c}{f_{fu}} \left[0.68 \frac{x_{\min}}{d_f} + 0.85 \frac{h_o}{d_f} \left(\frac{b}{b_o} - 1 \right) \right] + \rho'_s \frac{f'_s}{f_{fu}} - \rho_s \frac{f_y}{f_{fu}} \quad (38)$$

where x_{\min} and f'_s are respectively given by Eqs. (12) and (21).

4.2.2. Maximum FRP Reinforcement Ratio in Doubly RC "T" Section

$$\rho_{f \max} = \frac{f'_c}{f_{fbal}} \left[0.68 \frac{x_{bal}}{d_f} + 0.85 \frac{h_o}{d_f} \left(\frac{b}{b_o} - 1 \right) \right] + \rho'_s \frac{f'_s}{f_{fbal}} - \rho_s \frac{f_y}{f_{fbal}} \quad (39)$$

where x_{bal} , f_{fbal} and f'_s are respectively given by Eqs. (14), (23) and (24). To ensure a pseudo-ductile failure type, the FRP ratio is limited to:

$$\rho_f \leq \rho_{f \max} = 0.75 \rho_{f \max} \quad (40)$$

5. Capacity Curves

In considering the equilibrium of the section, the ultimate moment of resistance M_r must be greater or equal to the applied moment M_u therefore in Eqs. 4, 8, 25, and 31, μ_r is replaced by μ_s where: $\mu_s = \frac{M_u}{b_o d_f^2 f'_c}$.

An iterative procedure was adopted to determine the FRP ratio ρ_f for each assumed values of ρ_s and μ_s . The following flowchart resumes the different steps to be carried out to perform the various calculations. For the purpose of illustration, design graphs for both cases singly and doubly reinforced concrete rectangular and "T" sections are respectively shown in Figs. 4, 7 and 8 with:

$$b_o = 0.3, \quad \frac{b}{b_o} = 3.33, \quad \frac{h_o}{d_f} = 0.1, \quad \frac{d}{d_f} = 0.9, \quad f_y = 400 \text{ MPa},$$

$f'_c = 30 \text{ MPa}$, $\rho'_s = 0.23$ and 0.5% respectively for doubly rectangular and "T" sections. The exam of Figures 4-10 show that:

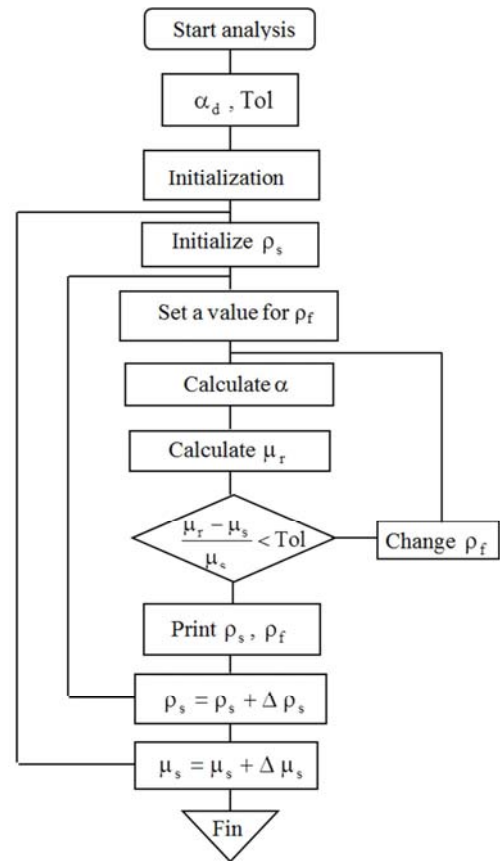


Figure 3. Flowchart of the design procedure of FRP strengthened sections.

- The ultimate flexural capacity of reinforced concrete "T" is significantly increased with the increase of FRP strips.
- This effect is more pronounced in beams having relatively small steel reinforcement ratio ρ_s .
- The rate of increase in ultimate flexural capacity

decreases as the FRP ratio is increased.

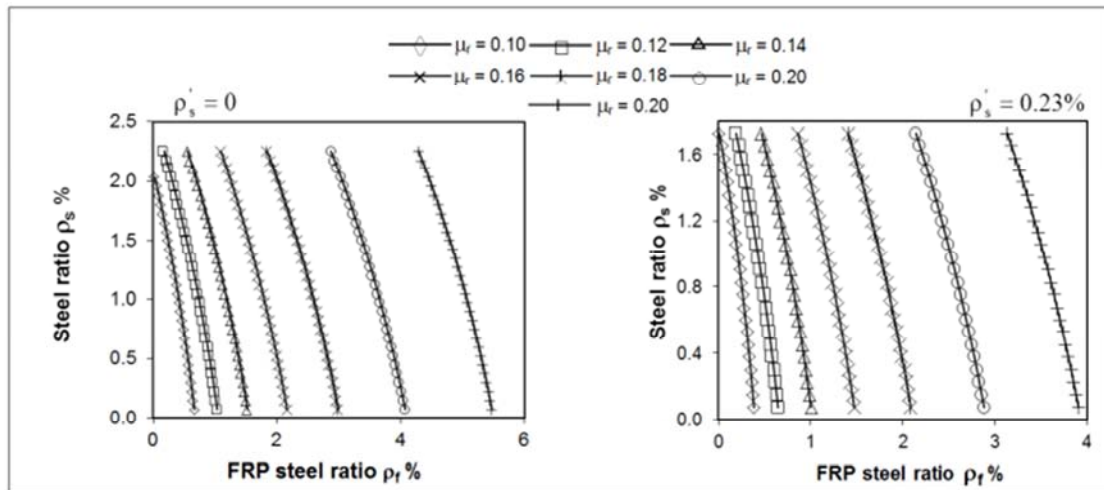


Figure 4. Design curves for FRP singly and doubly RC rectangular section.

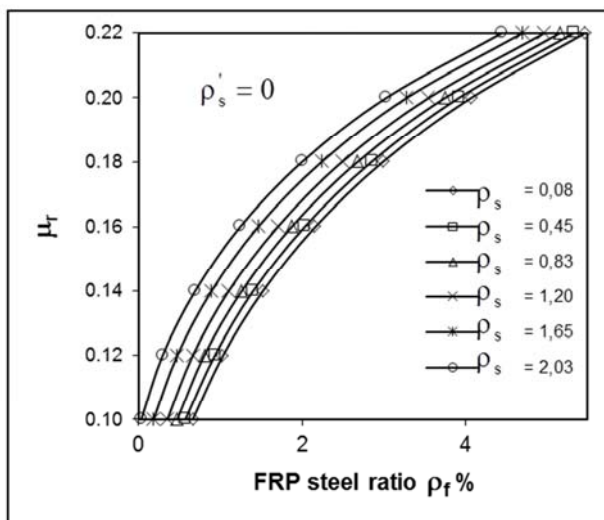


Figure 5. Flexural capacity curves for FRP singly RC rectangular section (ρ_s in %).

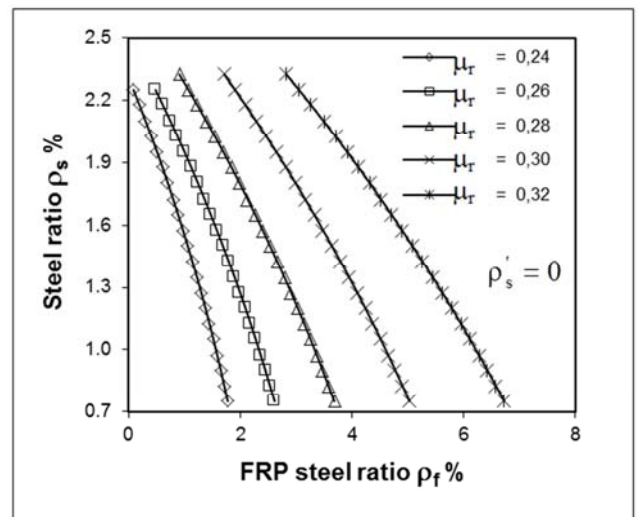


Figure 7. Design curves for FRP singly RC T-section.

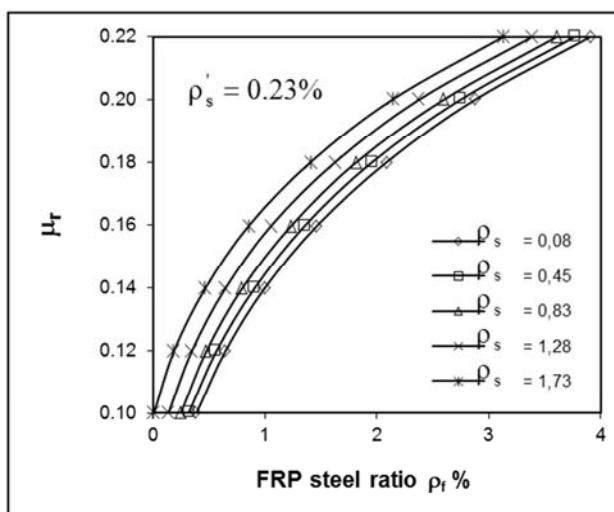


Figure 6. Flexural capacity curves for FRP doubly RC rectangular section (ρ_s in %).

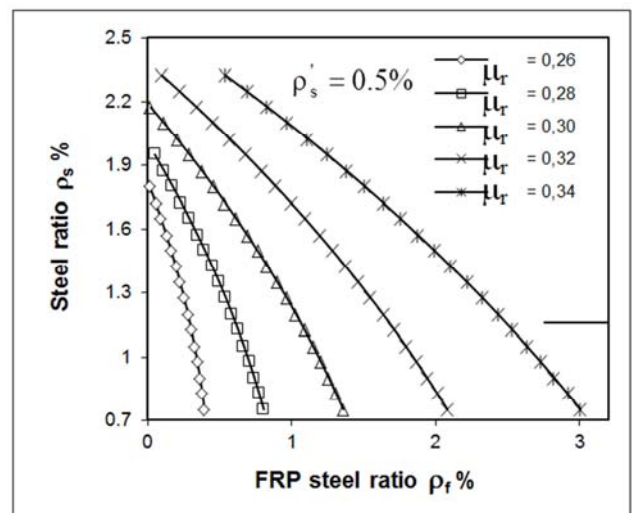


Figure 8. Design curves for FRP singly RC T-section.

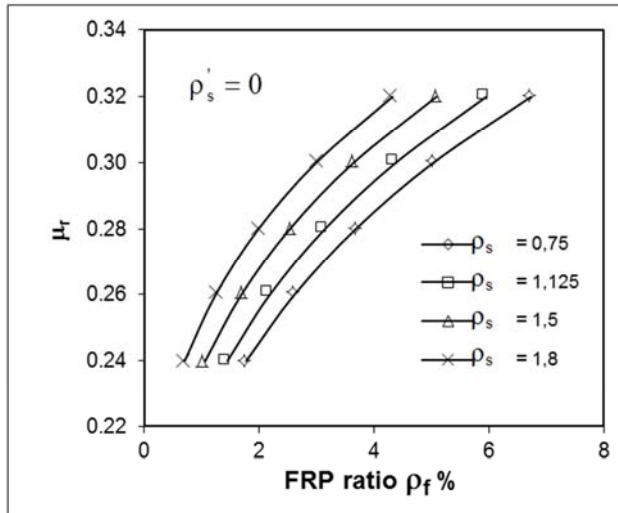


Figure 9. Flexural capacity curves for FRP singly RC T-section (ρ_s in %).

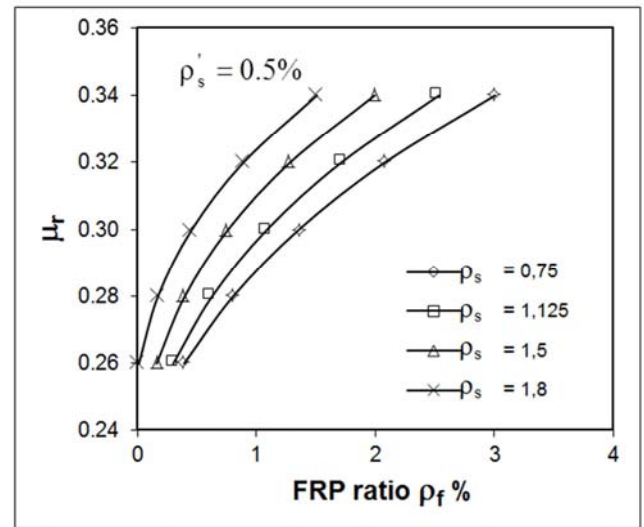


Figure 10. Flexural capacity curves for FRP doubly RC T-section (ρ_s in %).

6. Section Analysis Verification

Most of the experimental results available on this topic do not provide all parameters values so as to perform calculations for comparisons purposes. The results published by Barros (2005) indicate fortunately all the details regarding tested specimens and materials. A comparison is therefore made and the results are summarized in Table 1. All beams were tested in four-point bending over a simple span length.

Table 1. Comparison of results.

Beam	b_0 (mm)	d (mm)	A_s (mm ²)	A_s' (mm ²)	f_y (MPa)	f_y' (MPa)	f_{c28} (MPa)	A_f (mm ²)	E_f (GPa)	$P_{u \text{ Exp.}}$ (kN)	$P_{u \text{ Theo.}}$ (kN)	$P_{u \text{ Exp}} / P_{u \text{ Theo}}$
V2R2	100	152	339	402	730	530	48	28.5	160	78.5	75.8	1.035
V3R2	100	150	427	402	730	530	43	28.5	160	81.9	83.7	0.978
V4R3	100	155	603	402	730	530	46	42.75	160	94.9	114.1	0.832

7. Conclusions

A direct approach providing calculation simplicity for designing reinforced concrete rectangular and "T" sections strengthened with externally bonded NSM-FRP laminates based upon equilibrium and strain compatibility was presented. The equations developed are seamlessly utilized to design both simply and doubly reinforced concrete rectangular and "T" sections. It is important to note that the proposed relationships are valid for the case of FRP-NSM technique and that the debonding effect is not taken into account. Design graphs to facilitate implementation of the procedure were also developed. Upper and lower limits for FRP strip cross-sectional area to ensure ductile behavior of the strengthened beams were introduced.

The ultimate load represents the sum of the two equal concentrated loads applied to the beams at failure. The absolute average percent difference between the experimental ultimate loads and the theoretical ultimate loads predicted by the section analysis procedure was 94.8%.

These results clearly indicate that the analytical model is quite accurate in predicting the ultimate flexural capacity of reinforced concrete beams strengthened with NSM-FRP strips.

References

- [1] An W.; Saadatmanesh H.; Ehasani M. R. (1991), "RC beams strengthened with FRP plates. II: analysis and parametric study" Journal of structural engineering 117 (11): 3434-3455
- [2] Meier U.; Kaiser H. (1991), "Strengthening structures with CFRP laminates" In Proceedings, Advanced Composite Materials in Civil Engineering Structures, ASCE, New York, 224-232.
- [3] Sharif A.; Al-Sulaimani G. J.; Basunbul I. A.; Baluch M. H.; Ghaleb B. N. (1994), "Strengthening of initially loaded reinforced concrete beams using FRP plates" ACI Structural journal 91(2): 160-168.
- [4] Ross C. A.; Jerome D. M.; Tedesco J. W.; Hughes M. L. (1999), "Strengthening of reinforced concrete beams with externally composite laminates" ACI Structural journal 96 (2): 212-220.
- [5] Lamanna A. J.; Bank L. C.; Scott D. W. (2004), "Flexural strengthening of RC beams by mechanically attaching FRP strips" Journal of Composite for Construction 8 (3): 203-10.
- [6] El-Hacha R.; Rizkalla S. H. (2004), "Near-surface-mounted fiber-reinforced polymer reinforcements for flexural strengthening of concrete structures" ACI Structural journal 101(5): 717-26.

- [7] Barros J. A. O.; Fortes A. S. (2004), "Flexural strengthening of concrete beams with CFRP laminates bonded into slits" *Cement and Concrete Composites* 27 (4): 471-480.
- [8] Chikh N.; Merdas A.; Laraba A.; Benzaid R. (2013), "Study of the bond behavior of concrete beam strengthened with NSM-CFRP" *Lecture Notes in Engineering and Computer Science*, Volume 3 LNECS: 1815-1820.
- [9] Nguyen D. M.; Chan T. K.; Cheong H. K. (2001), "Brittle Failure and Bond Development Length of CFRP-Concrete Beams" *Journal of Composites for Construction*, ASCE, 5 (1): 7-12.
- [10] Mukhopadhyaya P.; Swamy N. (2001), "Interface shear stress: a new design criterion for plate debonding" *Journal of Composites for Construction*, ASCE, 5(1), 35-43.
- [11] Banijamalia S. M.; Esfahani M. R.; Nosratollahi S.; Sohrabi R.; Mousavi S. R. (2015), "Reviewing the FRP strengthening systems" *American Journal of Civil Engineering* 3 (2-2): 38-43.
- [12] Sayed Ahmad F.; Foret G.; Le Roy R. (2011), "Bond between carbon fibre reinforced polymer (CFRP) bars and ultra high performance fibre reinforced concrete (UHPFRC): Experimental study", *Construction and Building Materials* 25: 479-485.
- [13] Barros J. A. O.; Fortes A. S. (2002), "Concrete beams reinforced with carbon laminates bonded into slits", in *Proceedings of 5th Congreso de Métodos Numéricos en Ingeniería*, Madrid, Spain, 1-6.
- [14] De Lorenzis L.; Teng J. G. (2007), "Near-surface mounted FRP reinforcement: An emerging technique for strengthening structures. *Composites Part B Engineering*, 38(2): 119-143.
- [15] Sena-Cruz J.; Barros J.; Bianco V.; Bilotta A.; Bournas D.; Ceroni F.; Dalfré G.; Kotynia R.; Monti G.; Nigro E.; Triantafillou T. (2015), "NSM systems" In: *Design procedures for the use of composites in strengthening of reinforced concrete structures*, Pellegrino C.; and J. Sena-Cruz J. (eds.), RILEM State-of-the-Art Reports 19, Chapter 8: 303-348.
- [16] Kamiharako A.; Shimomura T.; Maruyama K.; Nishida H. (1999), "Stress transfer and peeling-off behaviour of continuous fiber reinforced sheet-concrete system". In *Proceedings, 7th East Asia-Pacific Conference on Structural Engineering and Construction*; Tokyo, 1283-1288.
- [17] Sena-Cruz J.; Barros J. A. O.; Gettu R. (2004), "Bond behavior of nearsurface mounted CFRP laminate strips under monotonic and cyclic loading." *Report DEC/E-04*, Department of Civil Engineering, University of Minho, Guimaraes, Portugal, 55 p.
- [18] Al-Mahmoud F.; Castel A.; François R. I.; Tournier C. (2010), "RC beams strengthened with NSM CFRP rods and modeling of peeling-off failure", *Composite Structures*, 92: 1923-1930.
- [19] Sayed Ahmad F.; Foret G.; Le Roy R. (2011) "Bond between carbon fibre reinforced polymer (CFRP) bars and ultra high performance fibre reinforced concrete (UHPFRC): Experimental study", *Construction and Building Materials* 25: 479-485.
- [20] Jung W-T.; Park J-S.; Kang J-Y.; Keum M-S. (2017), "Flexural behavior of concrete beam strengthened by Near-Surface Mounted CFRP reinforcement using equivalent section model" *Advances in Materials Science and Engineering*, Article ID 9180624, 16 pages. <https://doi.org/10.1155/2017/9180624>.
- [21] Picard A.; Massicote, B.; Boucher, E. (1999), "Strengthening of reinforced concrete beams with externally composite laminates" *ACI Structural journal* 96 (2): 212-220.
- [22] Malek A. M.; Saadatmanesh H. (1998), "Design equations and guidelines for RC beams strengthened with FRP plates" In *Proceedings of the 2nd International Conferences on Composites in Infrastructure*. University of Arizona, Tucson, Ariz, 603-617.
- [23] El-Mihilmy M. T.; Tedesco J. W. (2000), "Analysis of reinforced concrete beams strengthened with FRP laminates" *Journal of structural engineering* 126 (6): 684-691.
- [24] Almusallam T. H.; Al-Sallom Y. A. (2001), "Ultimate strength prediction for RC beams externally strengthened by composite materials" *Composites: Part B* 32 (7): 609-619.
- [25] Rasheed H. A.; Pervaiz S. (2003), "Closed form equations for FRP flexural strengthening design of RC beams" *Composites, Part B* 34 (6): 539-550.
- [26] Kang J-Y.; Park Y-H.; Park J-S.; You Y-J.; Jung W-T. (2005), "Analytical evaluation of RC beams strengthened with near surface mounted CFRP laminates" In *Proceedings of the 7th international symposium on fiber reinforced polymer reinforcement for reinforced concrete structures- FRP7RCS*, Kansas City, Missouri, November 7-10, 779-94.
- [27] Pesic N.; Pilakoutas, K. (2005), "Flexural analysis and design of reinforced concrete beams with externally bonded reinforcement" *Materials and Structures* 38 (2): 183-192.
- [28] Barros J. A. O.; Dias S. J. E.; Lima J. L. T. (2007), "Efficacy of CFRP-based techniques for the flexural and shear strengthening of concrete beams" *Cement and Concrete Composites* 29 (3): 203-217.
- [29] Teng J. G.; De Lorenzis L.; Wang B.; Li R.; Wong T. N.; Lam L. (2006), "Debonding Failures of RC Beams Strengthened with Near Surface Mounted CFRP Strips" *Journal of Composites for Construction* 2 (10): 92-105.
- [30] Hassan T.; Rizkalla S. (2002), "Flexural strengthening of prestressed bridge slabs with FRP systems" *PCI J.* 47(1), 76-93.
- [31] El-Hacha R.; Rizkalla S. H. (2004), "Near-surface-mounted fiber-reinforced polymer reinforcements for flexural strengthening of concrete structures" *ACI Structural Journal*, 101(5): 717-726.
- [32] Blaschko M. (2003), "Bond behaviour of CFRP strips glued into slits" In *Proceeding of the Sixth International Symposium on FRP Reinforcement for Concrete Structures (FRPRCS-6)*, K. H. Tan, ed., World Scientific, Singapore, 205-214.
- [33] De Lorenzis L. (2004), "Anchorage length of near-surface mounted fiber-reinforced polymer rods for concrete strengthening-analytical modeling" *ACI Structural Journal* 101(3): 375-386.
- [34] Coelho M. R. F.; Sena-Cruz J. M.; Neves L. A. C. (2015), "A review on the bond behavior of FRP NSM systems in concrete" *Construction and Building Materials*, 15 (93): 1157-1169.

- [35] Grace N. F.; Sayed G. A.; Soliman A. K.; Saleh K. R. (1999), "Strengthening of reinforced concrete beams using fiber reinforced polymer (FRP) laminates" *ACI Journal of Structures* 96 (5): 865-874.
- [36] El-Hacha R.; da Silva Filho J. N.; Melo G. S.; Rizkalla S. H. (2004), "Effectiveness of near surface mounted FRP reinforcement for flexural strengthening of reinforced concrete beams" 4th International Conference on Advanced Composite Materials in Bridges and Structures, Calgary, Alberta, July 20-23.
- [37] CBA 93. Algerian concrete code (Code du Béton Algérien-CGS Alger), Alegria, 1993. 200p. (in French).
- [38] ACI 318-02, Building code requirements for structural concrete. Detroit, Michigan: American Concrete Institute, 2002. 443p.